JOURNAL OF MATERIALS SCIENCE 28 (1993) 4375–4382

Nickel-based, binary-composite electrocatalysts for the cathodes in the energy-efficient industrial production of hydrogen from alkaline-water electrolytic cells

I. ARUL RAJ
Fuel Cells Division, Central Electrochemical Research Institute, Karaikudi-623 006, India

Ni–Mo, Ni–Zn, Ni–Co, Ni–W, Ni–Cr and Ni–Fe, binary-composite, codeposit surface coatings on mild-steel substrates were prepared by conventional electrodeposition techniques. The chemical compositions and the micrographic surface features of these coatings are reported. The utility of these coatings as cathodes in laboratory-scale alkaline-water electrolytic cells was assessed by polarisation techniques. The trend in their electrocatalytic activities ranks in this order: Ni–Mo > Ni–Zn > Ni–Co > Ni–W > Ni–Fe > Ni–Cr. The electrocatalytic activity of these coatings is very significant when compared with the data on conventional mild-steel cathodes currently used in industry. The results obtained experimentally are presented. A brief discussion is also included to highlight their utility.

1. Introduction

Research to evolve electrocatalysts based on transition metals for hydrogen-evolution reaction (HER) from alkaline-water electrolysis has drawn the attention of several scientists in recent years, owing to their concern over the conservation of the electrical energy associated with this process [1–11]. In tune with this international approach, and in continuation of my search for efficient and reliably performing materials for HER in an alkaline medium [12–14], keeping in view that present industrial cells use mild steel as the hydrogen-evolving cathode and work with a very low energy efficiency (50%), the experimental results obtained on the preparation of nickel-based, binary-surface coatings on suitably prepared mild-steel substrates by electrodeposition techniques and the performance of these coatings as catalytic cathodes for HER are presented and discussed in this paper.

2. Experimental procedure

2.1. Surface pretreatment of mild steel

Mild-steel foils with composition C = 0.06%, Si = 0.04%, Mn = 0.3%, P = 0.002%, Cr = 0.003%, Ni = 0.008% and Mo = 0.006% were sized into 20 cm by 5 cm rectangular strips. The shearing edges of the strips were machined to a smooth finish. The pretreatment procedure involved initial mechanical surface polishing to a mirror finish employing a fine emery cloth (John Oakey). This was followed by sand blasting of the surfaces with very fine sand particles. Then the surfaces were washed, dried and thoroughly degreased with acetone followed by washing with triple-distilled water. The surfaces were electrochemically polished by subjecting these pretreated strips to cathodic cleaning in an alkaline bath containing 40% sodium hydroxide, 10% sodium silicate and 10% sodium phosphate at 353 K and a current density of 100 mA cm^{-2} for 3 min. This was followed by anodic cleaning at the same conditions and more cathodic cleaning under the same conditions. Each substrate was then thoroughly washed with triple-distilled water to clean any embedded particles from the surfaces.

2.2. Codeposition processes

The electrolytic codeposition processes were carried out using a geometric area of 65 cm^2 on each side (130 cm^2 in total), masking the rest of the substrate surfaces with an alkali-resistant epoxy resin. A galvanostatic, steady-state deposition method was adopted, using two thin rectangular graphite strips as anodes, on both sides of the cathodes. The anodes were contained in nylon bags. The compositions of the electrolytic codeposition baths, the values of the codeposition variables adapted in this investigation and some physical data corresponding to the individual coatings are presented in Table I. The bath solutions were cleaned with activated charcoal followed by cathode dumming prior to their use, in order not to allow any trace impurities. The chemicals used were all of analar grade.

2.3. SEM, XRD and AAS experiments

The surface microstructures of the coatings were investigated by scanning electron microscopy (SEM, JOEL JSM 35 CF). The chemical composition of each codeposit was obtained by electron probe microanal-

0022–2461

TABLE I Operating conditions and bath characteristics for electrolytic codeposition

Parameters	Ni–Mo	Ni–W	Ni–Zn	Ni–Fe	Ni–Co	Ni-Cr
pH	10.5	10.5	5.5–6.5	10.5	10.5	10.5
Temperature (K)	301	301	333	301	301	301
Current density (mA cm^{-2})	10	10	5	10	10	10
Duration (min)	90	90	90	90	90	90
Agitation (r.p.m.)	250	250	250	250	250	250
Weight of deposit (mg cm^{-2})	3.6	3	4	5.1	10–11	5.6
Thickness of deposit (μm)	2.5–4.0	3.6	5–7	6–7	11–12	5-7
Colour of deposit	Grey	Pale black	Dull white	Pale grey	Black	Bright white
Adhesion	Very good	Very good	Very good	Good	Very good	Very good
$N_1SO_4 \cdot 6H_2O$ grams per litre (g.p.l.)	80	80	150	80	80	80
$FeSO_4 \cdot 7H_2O$ (g.p.l.)				20		
$K_3C_6H_5O_7 \cdot H_2O$ (g.p.l.)	50	50		50	50	Excess
Na_2CO_3 (g.p.l.)	Excess	Excess		Excess	Excess	Excess
$CoSO_4 \cdot 7H_2O$ (g.p.l.)					20	
CrO_3 (dil. HNO_3) (g.p.l.)						20
$Na_2MoO_4 \cdot 2H_2O$ (g.p.l.)	20					
$Na_2WO_4 \cdot 2H_2O$ (g.p.l.)		20				
$ZnSO_4 \cdot 7H_2O$ (g.p.l.)			40			
NH_4Cl			30			
CH_3COONa (g.p.l.)			30			
H_3BO_3 (g.p.l.)			15			

ysis (EPMA); The electron beam was fixed corresponding to the wave length of the metals under concern at a selected point on the corresponding coatings and also scanned over a wide area to record the degree of homogeneity from the EPMA spectrum.

An X-ray diffraction (XRD) study was made with CoK_α radiation (25 mA, 35 kV), in a range of 10 Hz, at a scan rate of 2° min^{-1} on a Ni–Mo coating, and the data derived from the diffraction pattern were compared with ASTM data.

The chemical compositions of the codeposit coatings were also estimated with a Perkin-Elmer Atomic Absorption Spectrophotometer (AAS Model 380) by chemical stripping of the coatings with acid solutions. The Ni–Fe coating was stripped by using a copper substrate instead of mild steel during codeposition.

2.4. Electrochemical polarisation experiments

The substrates coated with binary codeposits were designed as test cathodes for hydrogen evolution with exposed geometrical areas of 8.0 cm^2 by masking the remaining area with alkali-resistant epoxy resin. The polarisation experiments were carried out in a three-compartment stainless-steel cell under galvanostatic, steady-state conditions. Two nickel plates with a sufficiently large area, sacked in nylon bags, were used as auxiliary electrodes. The working cathodes under evaluation were separated from the anodes by a thin, commercial-grade, blue-asbestos cloth by wrapping the cathodes. A small hole was made in this cloth to ensure the closest contact between the cathodes and the reference electrode. As a reference, a Hg/HgO, OH^- electrode was used in the working solution, linked to the main compartment via a Luggin capillary. An alkaline solution (6 M) was prepared from analytical-grade KOH pellets in triple-distilled water and pre-electrolysed for 48 h at 100 mA cm^{-2} between two Pt electrodes in order to eliminate any electroactive impurities. The working electrodes were precathodized at 1 mA cm^{-2} for 30 min at room temperature. The open-circuit potentials were measured after 60 min at equilibrium conditions. Galvanostatic, steady-state potential values were measured as a function of applied current densities. These potential values were compensated for an *IR* contribution by an interruptor method. The *IR*-corrected potential values were used for the construction of Tafel plots. The kinetic parameters for the HER were derived from these plots.

2.5. Potentiodynamic experiments

Potentiodynamic experiments were carried out with a PAR Model 370 Electrochemistry System. An accelerated experiment [15] was adapted to assess the stability of these codeposit surface coatings. This involved reverse-potential cycling (RPC) of a precathodized electrode potentiodynamically. The cathodes were subjected to anodic scanning from their reversible hydrogen electrode potential (RHEP) values to − 0.740 V with respect to the Hg/HgO, OH^- electrode, at a scan rate of 0.5 mV s^{-1}. The scan was then reversed at the same rate to − 1.040 V. This cycling was continued until a significant change in the behaviour was observed. A plot of the anodic limiting currents, observed at − 0.85 V, was constructed as a function of the number of cycles.

2.6. Time-variation effects

Here, the experiments were carried out in a three-compartment, 10 dm^3 capacity, stainless-steel tank containing 8 dm^3 of the same alkaline solution. The time effects on the cathode potential values were studied by applying a constant cathodic current density for a long time with periodic replenishment of the electrolyte by triple-distilled water to restore the original volume, balancing the water that was lost due to

evaporation and electrolysis. Accelerated life tests were carried out by suddenly raising the current density to a specific value at regular time intervals of 5 days and monitoring the shift in the potential with time for 5 h. A few simulation experiments were also carried out by subjecting the coated cathodes to typical industrial-duty conditions. The electrical circuit was interrupted over time intervals ranging from 5 to 10 days and closed again to assess the effect of such severe, accidental or deliberate, incidents on the performance of the Ni–Mo coating, which was identified as the best among the present group of coated cathodes.

2.7. Thermal-activation experiments

As inclusion codeposits are likely in any electrolytic codeposition involving transition metals, such as Mo and W [16] the thermal activation of such systems at high temperatures in a hydrogen atmosphere was found [17] to improve their catalytic properties. Hence, the coated samples were laid down in an alumina tube, placed inside a glove box made of stainless steel and subjected to thermal activation in a hydrogen atmosphere in the temperature range 573–1073 K for various times. The effect of this treatment on the catalytic properties was studied by subjecting the thermally activated coatings to a constant cathodic current density of 300 mA cm^{-2} at typical electrolytic-cell-operation conditions for 6 h and then measuring the potential at the end of this period. The data were obtained by testing three identical test cathodes in each category. The potential values were not compensated for *IR*.

3. Results

3.1. Physical characteristics of the coatings

The average thickness of the binary coatings ranged from 2.5 to 12.0 μm. The average weight of the coatings ranged from 3.0 to 11.0 mg cm^{-2}. The adhesion of the coatings to the mild-steel substrates was very good. The XRD data obtained on Ni–Mo and Ni–W coatings is presented in Table II. The data indicate evidence for the formation of some new phases. Although the feasibility of codeposition of metals like Mo, W, Co, Fe, Zn and Cr along with Ni was well established [18–22], in the present work, an alkaline-citrate bath was employed under identical conditions to obtain all these coatings, except the Ni–Zn coating which was obtained from an acidic bath, for want of stability with an alkaline bath. Both ammoniacal baths and acid-citrate baths were also employed in the initial efforts but with little success. As it was known that Mo cannot be deposited from such aqueous solutions [23], it was hoped that the codeposition of Mo, with the other metals, could be induced by employing complex baths of the present formulation. As a whole, the physical characteristics of these binary coatings were sufficiently adequate to suit them for use as cathodes in electrolytic cells.

TABLE II XRD data obtained on Ni–Mo and Ni–W electrolytic codeposits

Codeposit	Measured d (nm)	ASTM value d (nm)	I/I_0	Phase
Nickel–molybdenum on mild steel	0.203	0.203	100	Ni
	0.134	0.133	40	$MoNi_4$
	0.117	0.116	50	
	0.265	0.272	40	
	0.143	0.140	5	MoO_3
Nickel–tungsten on mild steel	0.203	0.203	100	Ni
	0.156	0.158	76	W
	0.174	0.172	65	WO_2

3.2. Chemical compositions of the coatings

The EPMA results show a regular distribution of the metals in each of the coatings. The relative chemical compositions of the binary codeposit coatings were found to be 75% Ni and 20% Mo, for Ni–Mo; 80% Ni and 18% Fe for Ni–Fe; 54% Ni and 45% Co for Ni–Co; 73% Ni and 25% W for Ni–W; 60% Ni and 40% Zn for Ni–Zn; and 90% Ni and 7% Cr for Ni–Cr (in percentages of their gram-atomic weights). In the cases of Ni–Mo and Ni–W coatings, the presence of inclusion codeposits of MoO_3 and WO_2, respectively, is also brought out by the XRD data.

3.3. Micrographic structures of the coatings

SEM micrographs of the binary codeposit coatings (namely, Ni–Mo, Ni–Zn, Ni–Co, Ni–W, Ni–Fe and Ni–Cr) are shown in Fig. 1. These pictures show uniform microstructures, in general. They reveal evidence for stress with fine cracks. The grain sizes are not regular.

3.4. Cathode characteristics of the coatings

3.4.1. The reversible potential values

The reversible open-circuit potential values measured on these coated cathodes ranged from − 905 to − 960 mV, as shown in Table III. A negative temperature coefficient for the potential values was observed on all the cathodes. However, the values corresponding to the individual cathodes differ from each other, indicative of variation in their surface hydrogen coverage under equilibrium conditions. Even then, the values obtained were cathodic with respect to the theoretical value of a reversible hydrogen electrode in an alkaline medium under identical measurement conditions.

3.4.2. Electrochemical polarisation data

Tafel plots obtained for the coated cathodes for HER in 6 M KOH are shown in Figs 2 to 7. There are two different Tafel lines with distinct slopes for all the cathodes. The apparent values of the Tafel slopes, apparent values of the energy of activation obtained from Arrhenius-type plots (not shown) and hydrogen-overpotential values (η_{H_2}) derived from these plots are presented in Table IV. At very low current density

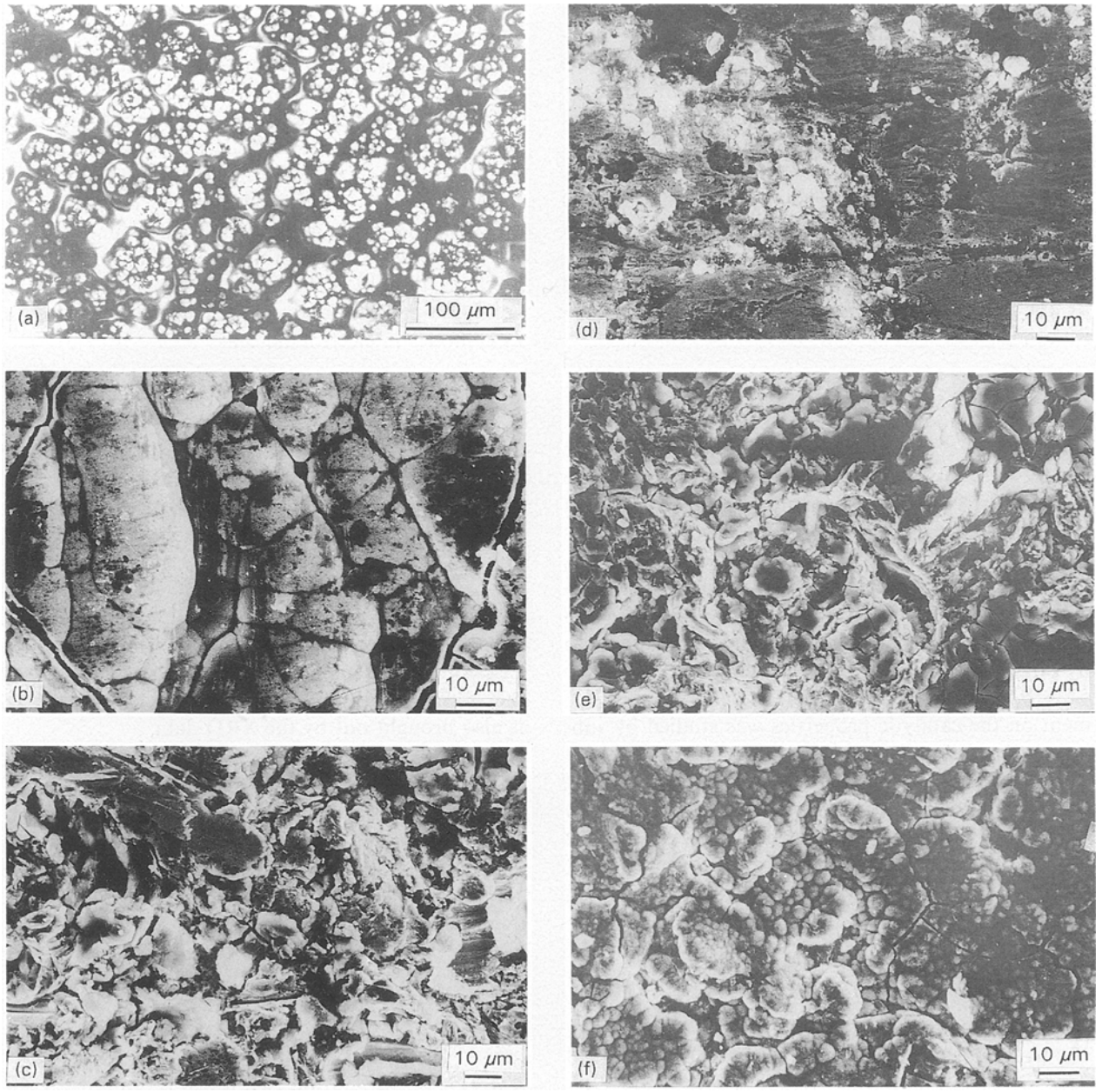

Figure 1 SEM micrographs of binary codeposit coatings: (a) Ni–Mo, (b) Ni–Zn, (c) Ni–Co, (d) Ni–W, (e) Ni–Fe, and (f) Ni–Cr.

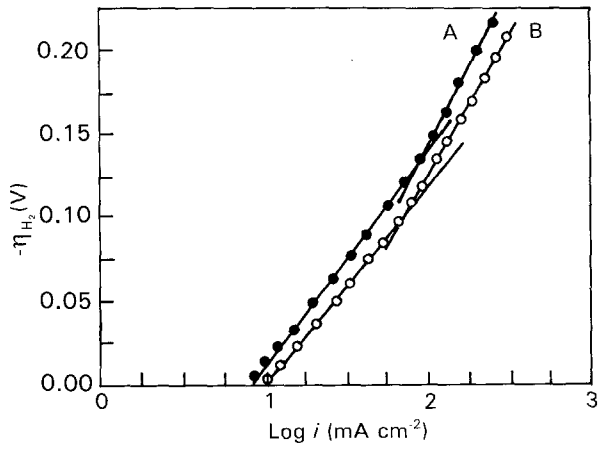

Figure 2 Tafel plot for the HER on the Ni–Mo coated cathode in 6 M KOH: (A) 303 K, and (B) 353 K.

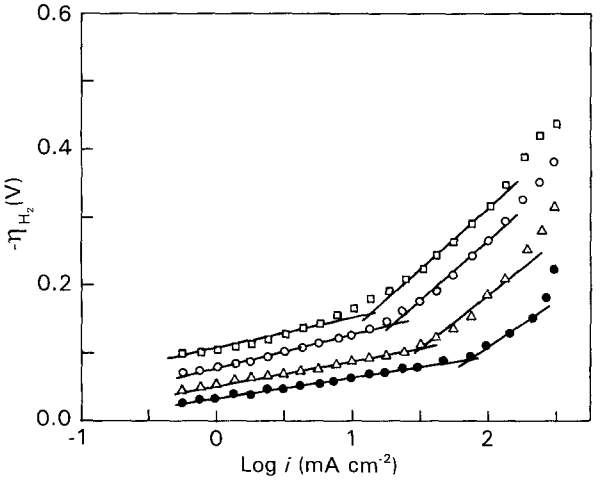

Figure 3 Tafel plot for the HER on the Ni–Zn coated cathode in 6 M KOH: (●) 353 K, (△) 333 K, (○) 318 K and (□) 303 K.

TABLE III The reversible open-circuit cathode potentials of Ni–based binary codeposits in a 6 M KOH solution

Codeposit	Potential[a] (mV)	Temperature (K)
Ni–Mo	– 960	303
	– 957	318
	– 954	333
	– 951	353
Ni–Zn (after leaching Zn in KOH)	– 947	305
	– 942	318
	– 936	333
	– 929	353
Ni–W	– 935	305
	– 922	318
	– 914	333
	– 905	353
Ni–Fe	– 951	305
	– 944	318
	– 940	333
	– 934	353
Ni–Co	– 939	305
	– 930	318
	– 922	333
	– 917	353
Ni–Cr	– 931	305
	– 919	318
	– 911	333
	– 907	353

[a] The potential is with respect to Hg/HgO, OH^- (6 M).

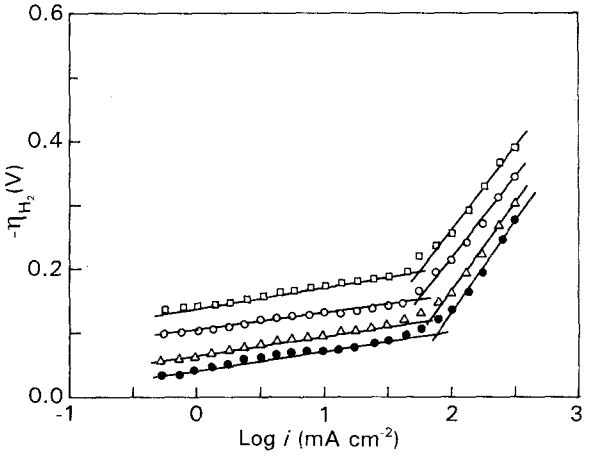

Figure 4 Tafel plot for the HER on the Ni–Co coated cathode in 6 M KOH: (●) 353 K, (△) 333 K, (○) 318 K, and (□) 303 K.

values, the polarisation of the Ni–Mo coated cathode was negligibly less and this region was, therefore, not included in Fig 2. This electrochemical data can only predict the trend in electrocatalytic activities, as there are deviations in the Tafel linearity at very high current densities ($i > 250$ mA cm^{-2}), owing to intensive surface coverage by the hydrogen bubbles evolved.

The following general points can be made for this data, including the data obtained for the mild-steel substrate as cathode for comparision.

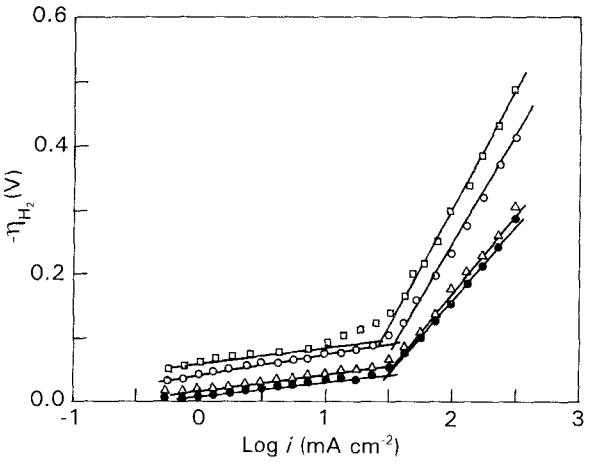

Figure 5 Tafel plot for the HER on the Ni–W coated cathode in 6 M KOH: (●) 353 K, (△) 333 K, (○) 318 K, and (□) 303 K.

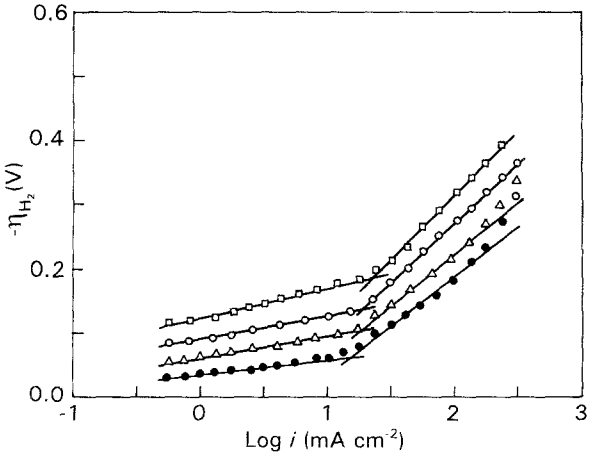

Figure 6 Tafel plot for the HER on the Ni–Fe coated cathode in 6 M KOH: (●) 353 K, (△) 333 K, (○) 318 K, and (□) 303 K.

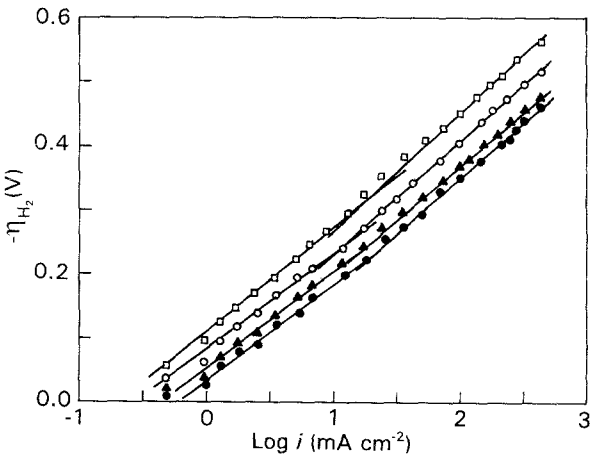

Figure 7 Tafel plot for the HER on the Ni–Cr coated cathode in 6 M KOH: (●) 353 K, (▲) 333 K, (○) 318 K, and (□) 303 K.

1. All the six binary coatings considered in this work exhibit electrocatalytic activity towards the HER in an alkaline medium when compared with mild steel.

2. The hydrogen overpotential under typical industrial conditions (300 mA cm^{-2} and 353 K) is 0.3 V

TABLE IV Electrochemical data for hydrogen evolution on codeposit cathodes in 6 M KOH

Codeposit	Temp. (K)	b(mV. dec^{-1})		Energy of activation (kJ mol^{-1})		$-\eta_{H_2}$ (mV) at 300 mA cm^{-2}
		At $i < 50$ mA cm^{-2}	At $i > 50$ mA cm^{-2}	At low η	At high η	
Ni–Mo	353	110	180	2.3	2.0	185
Ni–Zn	353	50	175	52.63	38.28	225
Ni–Fe	353	25	150	63.8	17.06	270
Ni–W	353	25	225	58.03	7.66	280
Ni–Co	353	35	245	109.3	24.22	240
Ni–Cr	353	150	170	22.17	19.49	445
Mild steel	353	135	125	59.8	68.1	540

less on the Ni–Mo coated cathode than the mild-steel cathode.

3. Dual Tafel slopes exist for all the coated cathodes and also for the mild-steel cathode (not shown).

4. The Tafel-slope values for the coatings (namely, Ni–Co, Ni–W, Ni–Zn and Ni–Fe) range from 30 to 50 mV dec^{-1} at low polarization conditions ($i < 50$ mA cm^{-2}). The values for Ni–Mo and Ni–Cr coated cathodes ranged from 110 to 150 mV dec^{-1} (per decade). At high polarisation conditions namely, $i > 50$ mA cm^{-2}), the values range from 135 to 190 mV dec^{-1} for Ni–Mo, Ni–Zn, Ni–Fe and Ni–Cr; the values for Ni–Co and Ni–W are greater than 200 mV dec^{-1}.

5. The apparent energy of activation values for HER obtained on these coated cathodes do not show any trend. However, the value for Ni–Mo is the lowest of all.

3.4.3. Reverse potential cycling data

Fig. 8 shows a graph of anodic limiting oxidation currents observed in the RPC experiments on these coated cathodes against the number of cycles in 6M KOH at 301 K and at -0.85 V. In general, these cathodes do not undergo oxidation up to $+200$ mV above the reversible hydrogen electrode potential (RHEP). It is also apparent that the oxidation currents do not vary on repeated cycling, indicating that these currents represent the oxidation of hydrogen evolved on the cathode during cathodic half cycles of the potentiodynamic scanning.

3.4.4. Time-variation effects

The time-variation effects on the present group of coated cathodes under typical industrial operation conditions were assessed and their electrochemical stability as a function of operation time is shown in Fig. 9. The Ni–Mo coated cathode shows an almost steady potential value up to 1500 h of continuous use as a cathode. The behaviour of the other coated cathodes with time shows that they do not retain their stability with time in continuous use.

3.4.5. Thermal-activation effects

The electrochemical data obtained after subjecting the coated cathodes to thermal activation in a protective hydrogen atmosphere is presented in Table V. This data indicates that, in general, the cathode-potentials are less cathodic on activated cathodes when compared with their corresponding unactivated counterparts. It is also evident that an optimum saving of 50 mV is realized on the Ni–Mo coated cathode. Activation at 1073 K for a long time does not do much.

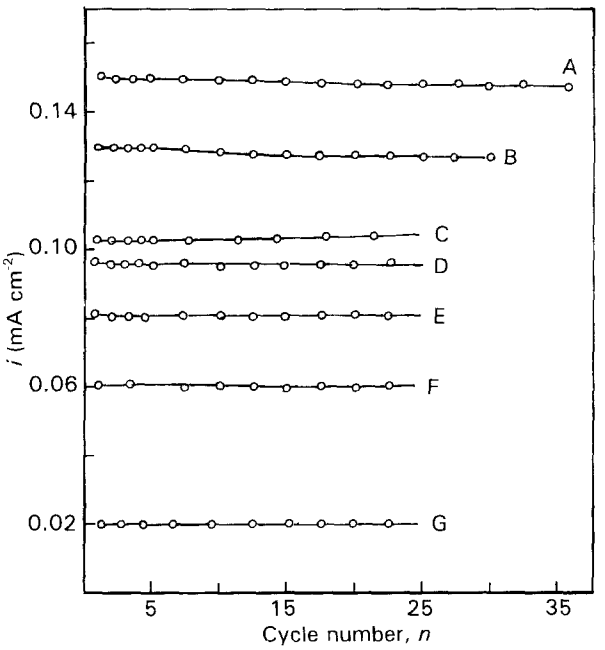

Figure 8 Plots of anodic limiting oxidation currents in the RPC tests versus number of cycles in 6 M KOH at 301 K and -0.85 V. (A) Ni–Mo, (B) Ni–W, (C) Ni–Co, (D) Ni–Fe, (E) Ni–Cr, (F) Ni–Zn, (G) Ni-plated mild steel.

3.4.6. Simulated life tests

The accelerated life tests carried out on the Ni–Mo coated cathode indicated that the variation in the cathode potential was 30 mV during a test period of 60 days at 600 mA cm^{-2} and at 353 K. The results obtained on other coated cathodes indicated a variation of 60 to 80 mV during a period of 10 days. The simulation experiments indicated a jump of 60 mV in the open-circuit potential value after an interruption period of 15 days on Ni–Mo cathodes. However, the original values were again established by subjecting them to very low cathodic currents (0.1 μA cm^{-2}) for 60 min.

TABLE V Effects of thermal activation in a hydrogen atmosphere on the catalytic activities of codeposit cathodes (E is not compensated for IR, and was obtained at 300 mA cm^{-2})

Codeposit	Temp. (K)	Duration (h)	$-E_{300}$ (mV) at 353 K
Ni–Mo	573	5	1134
	773	5	1125
	1073	5	1080
	1073	10	1077
	1173	10	1075
Ni–Zn (after leaching Zn in KOH)	1073	5	1140
	1073	10	1130
Ni–Co	1073	5	1180
	1073	10	1178
Ni–W	1073	5	1200
	1073	10	1185
Ni–Fe	1073	5	1225
	1073	10	1217
Ni–Cr	1073	5	1355
Ni-plated mild steel	1073	5	1420

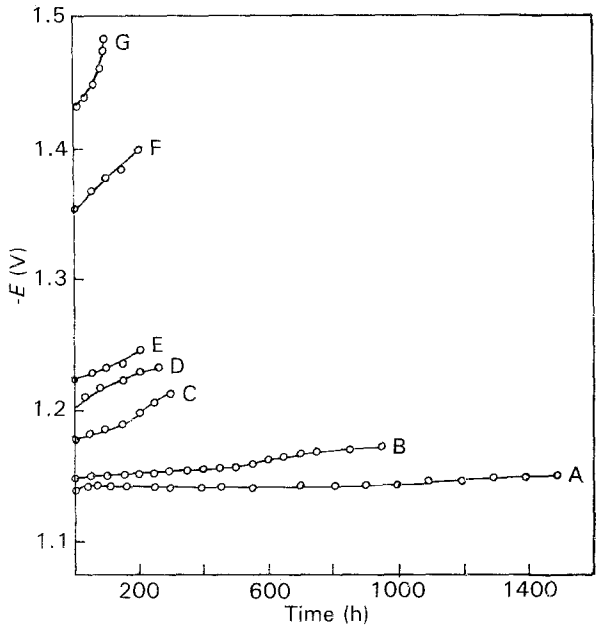

Figure 9 Time-variation effects on the cathode potentials at 353 K and at 300 mA cm^{-2} in 6 M KOH. (A) Ni–Mo, (B) Ni–Zn, (C) Ni–Co, (D) Ni–W, (E) Ni–Fe, (F) Ni–Cr, (G) Ni-plated mild steel.

4. Discussion

4.1. The magnitude of Tafel slopes

The Tafel slope values (30 to 50 mV dec^{-1}) obtained on Ni–Co, Ni–W, Ni–Zn and Ni–Fe binary-co-deposit-coated cathodes for HER at low polarisation conditions in an alkaline medium agree well with the values reported on other transition-metal-based coatings; that is, on Ni–Fe electrodeposits [24, 25] Ni–Mo thermal coatings [26] and Ni–Mo–Cd ternary electrolytic coatings [27, 28]. The Tafel-slope values on Ni–Mo, Ni–Cr cathodes (110–150 mV dec^{-1}) are not in agreement with the results of similar electrodes, for example, Ni–Mo–Cd cathodes [27, 28]. The very low values reported by these authors (30 to 38 mV dec^{-1}) were estimated in the current-density region from 0.01 mA cm^{-2} to 30 mA cm^{-2}. However, in review of the common, practical, alkaline-water electrolysis conditions, namely 300 mA $cm^{-2} > i > 10$ mA cm^{-2}, in the present work, the Tafel parameters were obtained under these conditions. The values obtained under high polarisation conditions ($i > 100$ mA cm^{-2}) vary significantly among these coated cathodes. Furthermore, no correlation exists between the d-band structures of the constituent metals and the ΔE values obtained experimentally.

4.2. Mechanistic aspects of HER

The value of the Tafel slope, 110 mV dec^{-1}, obtained for the Ni–Mo coated cathode agrees with the theoretical value, 120 mV dec^{-1}, predicted for the mechanism involving the first electron transfer (Volmer reaction) as the rate-determining step for a HER at low current densities. The values in the range 30–50 mV dec^{-1} obtained for the other coated cathodes agree with a mechanism involving fast discharge followed by rate-determining recombination of the absorbed hydrogen atoms (Heyrovsky reaction) step in the HER. At high current densities, the mechanism of a HER involves coupled-reaction sequences, and is not clear.

4.3. Hydrogen-overpotential values

From the results obtained in this work, the electrocatalytic activities of the present transition-metal-based binary coatings for the HER in an alkaline medium are found to rank in this order: Ni–Mo > Ni–Zn > Ni–Co > Ni–W > Ni–Fe > Ni–Cr. The Ni–Mo coated cathode had a hydrogen-overpotential value of 0.180 V after 1500 h of continuous operation in 6M KOH at 300 mA cm^{-2} and at 353 K, which is about 0.3 V less when compared with the value for the mild-steel cathode (0.540 V).

4.4. Practical utility of Ni–Mo coated cathodes

The results of the service life tests, thermal activation effects, and RPC experiments carried out on the Ni–Mo coated cathode indicate its adequate electrochemical stability for use in laboratory-scale, alkaline-water electrolytic cells. The hydrogen-overpotential value of 0.180 V on this coated cathode at typical, industrial, working conditions implies that this Ni–Mo is a potential catalyst for the HER from an alkaline medium. Furthermore, the replacement of the conventional mild-steel cathodes by Ni–Mo adds only a little to the cost. However, the energy saving that can be realised by this change, around 0.3 V, contributes significantly to the economy of the electrochemical production of hydrogen.

5. Conclusions

The following points form a summary of the results obtained in the present set of experiments

1. Ni–Mo, Ni–Zn, Ni–Fe, Ni–Co, Ni–W and Ni–Cr binary-composite, codeposit coatings can be prepared

conveniently on properly surface-prepared, mild-steel substrates employing the electrolytic baths reported in this work.

2. All these coatings exhibit electrocatalytic activity for the HER in an alkaline medium.

3. The Ni–Mo coated cathode is the best of the six coated cathodes investigated in this work.

4. The Ni–Mo coated cathode meets some of the requirements necessary for application as an electrocatalytic cathode in alkaline-water electrolytic cells.

5. The industrial application of this coated cathode can only be realised after subjecting large-size, sample Ni–Mo cathodes to commercial-scale cells.

Acknowledgements

The author is very grateful to Professor K. I. Vasu, the former director, and Professor S. K. Rangarajan, the present director, of the Central Electrochemical Research Institute, Karaikudi-6 for their constant encouragement.

References

1. D. E. BROWN, M. N. MAHMOOD, M. C. M. MAN and A. K. TURNER, *Electrochim Acta* **29** (1984) 1551.
2. M. R. GENNERO de CHIALVO and A. C. CHIALVO, *ibid.* **33** (1988) 825.
3. H. E. G. ROMMAL and P. J. MORAN, *J. Electrochem. Soc.* **126** (1985) 325.
4. J. Y. HUOT and L. BROSSARD, *Surf. Coat. Technol.* **34** (1988) 373.
5. L. VRACAR and B. E. CONWAY, *Electrochim. Acta* **15** (1990) 701.
6. E. POTVIN, H. MENARD, J. M. LALANCETTE and L. BROSSARD, *J. Appl. Electrochem.* **20** (1990) 252.
7. J. DIVESEK, P. MALINOWSKI, J. MERGEL and H. SCHMITZ, *Int. J. Hydrogen Energy* **13** (1988) 141.
8. M. M. JAKSIC, *Electrochim. Acta* **29** (1984) 1539.
9. *Idem., Int. J. Hydrogen Energy* **12** (1987) 727.
10. A. K. VIJH, R. JACQUES and G. BELANGER, *J. Prog. Batteries Solar Cells* **5** (1984) 255.
11. D. E. HALL, J. M. SARVER and D. O. GOTHARD, *Int. J. Hydrogen Energy* **13** (1988) 547.
12. I. ARUL RAJ and V. K. VENKATESAN, *Int. J. Hydrogen Energy* **13** (1988) 215.
13. I. ARUL RAJ and K. I. VASU, *J. Appl. Electrochem.* in press.
14. I. ARUL RAJ and V. K. VENKATESAN, *Trans. SAEST* **22** (1987) 189.
15. M. B. JANJUA and R. L. LE ROY, *Int. J. Hydrogen Energy* **10** (1985) 11.
16. A. BRENNER, in "Electrodeposition of alloys, principles and practice". Vol. 2, (Academic Press, New York 1963) p. 430.
17. H. WENDT and V. PLZAK, *Electrochim. Acta* **28** (1983) 27.
18. E. BELTOWSKA-LEHMAN and K. VU QUANG, *Surf. Coat. Technol.* **12** (1986) 75.
19. C. KARWAS and T. HEPEL, *J. Electrochem. Soc.* **135** (1988) 839.
20. D.E. HALL, *ibid.* **128** (1981) 740.
21. P. W. T. LU and S. SRINIVASAN, *ibid.* **125** (1978) 265.
22. B. TERESZKO, A. RISENKAMPF and K. VU QUANG, *Surf. Coat. Technol.* **12** (1981) 301.
23. A. T. WASKO, "Electrochimia molibdina i wolframa" (Izd. Naukowa Dunka, Kiev, 1977).
24. L. BROSSARD, *Int. J. Hydrogen Energy* **16** (1991) 13.
25. E. R. GONZALES, L. A. AVACA, A. CARUBELLI, A. A. TANAKA and G. TREMILIOSI-FILHO, *Int. J. Hydrogen Energy* **9** (1984) 689.
26. D. E. BROWN, M. N. MAHMOOD, A. K. TURNER, S. M. HALL and P. O. FOGARTY, *ibid.* **7** (1982) 405.
27. B. E. CONWAY, H. ANGERSTEIN-KOZLOWSKA, M. A. SATTAR and B. V. TILAK, *J. Electrochem. Soc.* **130** (1983) 1825.
28. B. E. CONWAY and L. BAL, *J. Chem. Soc., Faraday Trans. 1* **81** (1985) 1841.

Received 28 January
and accepted 17 November